2018 International Conference on Unmanned Aircraft Systems (ICUAS)
Dallas, TX, USA, June 12-15, 2018

Wind Measurement and Estimation with Small Unmanned Aerial Systems (sUAS) Using On-Board Mini Ultrasonic Anemometers

Derek Hollenbeck[1], Gregorio Nunez[1], Lance E. Christensen[2] and YangQuan Chen[1]

***Abstract*— Accurate and precise measurements of wind are important for understanding atmospheric transport, especially when trying to localize and quantify natural gas emissions from pipeline leaks. This work looks at the applicability of measuring wind speed and direction with mini ultrasonic anemometers on-board small unmanned aerial systems. The 'prop wash effect' from propeller air intake mixing of the wind is quantified through experiments for a multi-rotor platform in a low cost wind tunnel (LCWT). Trisonica and FT742SM sensors are compared through wind tunnel experiments for accuracy confirmation. The validation of measuring wind conditions on-board is compared with accepted estimation techniques for VTOL and fixed wing platforms.**

I. INTRODUCTION

The ability to measure wind speed and direction accurately can be a powerful tool when used in experiments that depend on micrometeorology such as detecting fugitive gases in the oil and gas pipeline industry. These fugitive gases are usually small and difficult to detect. Using an open path laser spectrometer(OPLS) on-board sUAS, developed by NASA JPL, it is possible to detect fugitive gases at ppb levels. In this application, it was shown that prop wash could be neglected if the sensor is placed in a region out in front of the aircraft by 8in. By flying or being in winds excess of $\approx$ 2m/s the OPLS could detect without recirculation or prop wash influence, which is defined as a propeller air intake mixing of the wind before the measurement [1]. The work now looks to improve fugitive methane localizations through improving wind speed and direction measurements. By making wind measurements in situ the local meteorology can be captured near the OPLS measurement. This is opposed to static weather station measurements that force the use of extrapolation or assumptions of a mean wind field. This is especially critical when flying around buildings to capture the local wind characteristics. There has been some efforts to measure on-board sUAS from Bruschi el al [2] using a MEMs based solid state anemometer. They showed that prop wash effect is significant at wind speeds less than 10m/s with wind direction being unaffected. Until recently, miniature wind sensors light enough to mount on-board haven't been readily available. Sensors like the Trisonica-Mini are now light enough to be used in this application but have yet to be explored or validated.

Wind estimation techniques have increased in sophistication over the years to improving navigation and control of aircraft (i.e. [3] [4]). Some examples include exponentially stable nonlinear observers [5], discrete time Kalman Filters [6], Sigma-point Filters (UKF) [7] [8], or a moving horizon estimator (MHE) [9]. These techniques are then challenged or validated through simulation and sometimes compared with weather station data through extrapolation of ground friction effects. The accuracy of these extrapolations of course depends on atmospheric stability, as well as the height of the weather station measurements, and the method itself (traditional power law, Mesonet-derived power law, neutral power law) [10]. This can present problems if you need accurate wind measurements at a specific location, especially when the data is to be used to model or predict events such as in flux measurements through the mass balance technique [11].

The focus and contribution of this paper will be on the application of light-weight mini ultrasonic anemometers on-board ready-to-fly (RTF) sUAS and how they compare with accepted wind estimation techniques. The paper is organized as follows. Section II discusses the platforms used. Section III goes over the sensors and wind tunnels used. Section IV goes over the placement of the sensors and the prop wash effect on the VTOL. Section V discusses the estimation techniques used. Section VI goes over the experiment which is then followed by the results (Section VII) and concluding remarks (Section VIII).

II. PLATFORMS

Two types of sUAS were considered: vertical take-off and landing (VTOL) as well as fixed-wing. The Foxtech Hover1 (VTOL) and 3DRobotics Aero (fixed-wing) were chosen due to their flight endurance, light-weight, low cost (<\$1000), and autonomous flight capabilities (see Fig. 1). Both platforms fall into the CFR 14 Part 107 small category sUAS.

The Foxtech Hover1 is equipped with 4, 15"x5.2" folding propellers and Tiger Motor MN3508 KV380 brush-less DC motors. The motors are powered by a 6S 9500 mAh LiPo battery with Foxtech Multi-Pal 40A OPTO electronic speed controller (ESC). It has a takeoff weight of 2.3kg and has been endurance tested for >45min flights with no load. The airworthiness limits the aircraft to winds less than 20 m/s and for our purposes we will further limit winds to 10 m/s for added safety. The flight controller is a Pixhawk2 autopilot

Correspondence should be sent to Derek Hollenbeck (dhollenbeck@ucmerced.edu) or Professor YangQuan Chen (ychen53@ucmerced.edu). DH was supported by NSF NRT Fellowship.

[1]Department of Mechanical Engineering, University of California, Merced, CA 95343, USA

[2]Jet Propulsion Laboratory, 4800 Oak Grove Drive Pasadena, CA 91109, USA

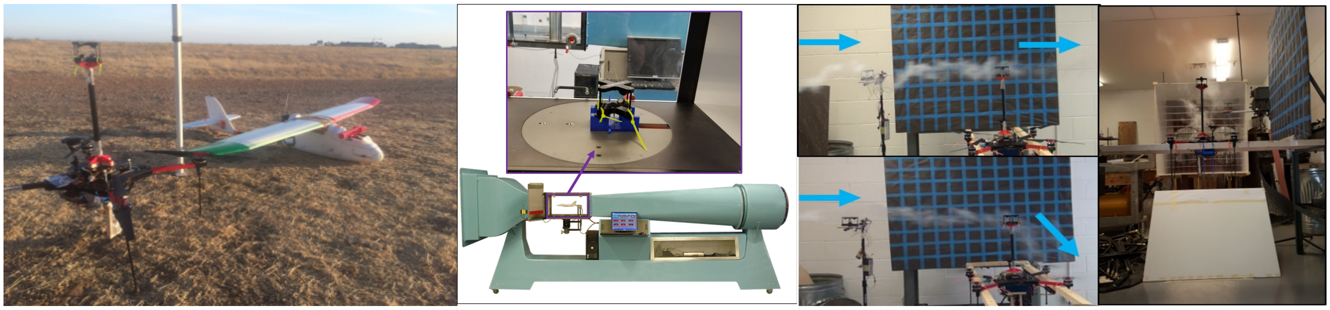

(a) (b) (c)

Fig. 1: (a) Platforms with the on-board Trisoncia-Mini anemometer (left) Hover1 (right) Aero (b) Shows mounting location inside the Aerolabs Educational Wind Tunnel (EWT) (c) The experimental setup to determine wind bias under controlled conditions.

system with a Here+ GNSS GPS receiver based on UBlox M8P. This GPS receiver has Real Time Kinematics (RTK) capabilities though it is not used in this work.

The Aero is a ready to fly (RTF) fixed-wing aircraft made by 3DRobotics equipped with a Pixhawk autopilot system. It has a 1,880mm wingspan and a single pusher style 11"x7" propeller powered by a Tiger motor 2820 KV830 motor. A digital airspeed sensor that uses a pitot-static tube and a differential pressure sensor (DPS). The flight time is 40 min with payload capacity of 4kg. The flight speed ranges from 12m/s (27mph) to 18m/s (40mph).

III. Sensors and Wind Tunnels

The Trisonica-Mini by Anemoment is one of the lightest (50g) ultrasonic anemometers on the market. It is capable of measuring wind speed with a stated accuracy of ±0.1m/s for winds speeds under 15m/s and a resolution of 0.1 m/s. Additionally, it measures wind direction in the horizontal plane (N,E) from 0-360° and the vertical plane (D) between $\pm30°$ both to an accuracy $\pm1.0°$ at 1.0° resolutions. This wind sensor can also provide temperature, humidity, pressure, tilt and compass measurements (heading accuracy of $\pm5.0°$). This technology uses the principle of time of flight which changes as a function of air velocity [12].

The FT742 SM (surface mount) by FT Technologies is a ruggedized acoustic resonance anemometer. It is capable of measuring wind speeds between 0 and 75 m/s with a stated accuracy of ±0.3m/s for winds speeds under 16m/s. The resolution of this measurement is on the order of 0.1 m/s. The wind direction can be measured with a 1° resolution and accuracy of 4° RMS. It also has a magnetometer with accuracy of 5° RMS. The principle of acoustic resonance in this sensor will automatically compensate for variations in temperature, pressure, and humidity [13].

The Aerolab EWT is a commercial wind tunnel designed for educational instruction providing good controlled range on airspeed and laminar flow. The test chamber is sealed and uses a negative pressure from exhaust to pull air through the system. The specifications can be seen in Table I with comparison to the low cost wind tunnel. The low cost wind tunnel (LCWT) was built from readily available materials and powered by two 1/2hp Global 30in pedestal fans with 3 blades. The inlet forms a nozzle to the straighteners followed by a 6 foot length of straight chamber to the exhaust. The speed settings on the fans can produce wind speeds of ~2.5m/s, ~3m/s, and ~3.4m/s with a standard deviation of ~.41m/s. The output velocity of the the LCWT is not fully laminar flow and contains some cyclic eddies.

TABLE I: Aerolab EWT Specifications

Item	Aerolab EWT	LCWT
Airspeed Range	4.5m/s - 65+m/s	2.5m/s - 3.4m/s
Turbulence Level	Less than 0.2%	± 0.5m/s
Test section	12"x12"x24"	open (3'8"x4')
Fan	9 blade	3 blade (x2)
Flow Straightener	4in deep honeycomb	4in deep blade
Turbulence Reducer	mesh screens	None

IV. Sensor Placement and Prop Wash Effect

The following experiments attempt to verify the sub-optimal placement of a wind sensor on-board a VTOL and fixed-wing aircraft, in particular the Hover1 and Aero.

To start we placed the Trisonica-Mini and FT742SM into the Aerolab EWT to check the accuracy and standard deviation (see Fig 1 (b)). We sampled three different Trisonica-Mini's and one FT742SM at eight different speeds each for a period of 1 min. The results from the Aerolab EWT (Fig. 2 (a) & (b)) showed a standard deviation between 0.1 and 0.3 m/s and in one case high variance and error in the Trisonica labeld T2. The FT742SM had the overall lowest error and standard deviation. To accommodate the Hover1 we then moved to the LCWT to investigate the effect of prop wash on the Trisonica. We assume impact of the prop wash on the sensor to be a function of the motor speed. The set up is as follows, Trisonica (T1) is fixed on-board the Hover1 while (T3) is placed in a location where the influence of prop-wash is negligibly small. The placement of (T1) was based on previous works [1]. This was found by using an AeroLab Smoke Generator, a device that expels smoke

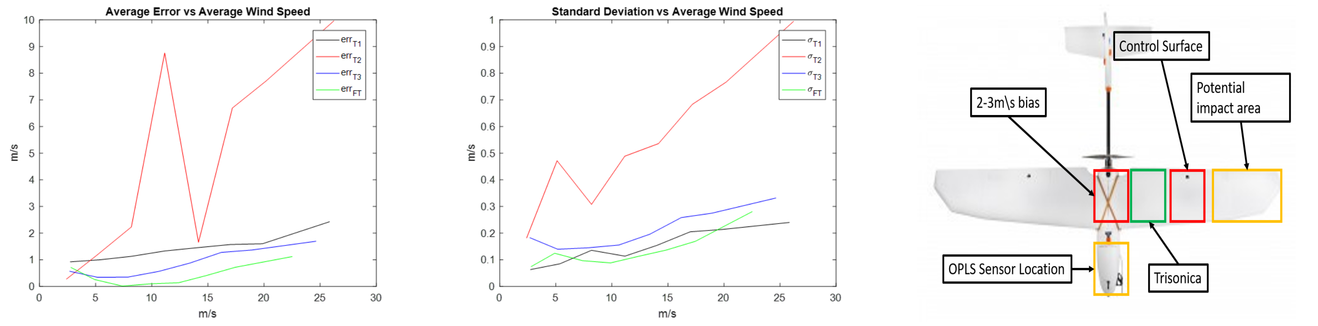

(a) (b) (c)

Fig. 2: Aerolab EWT results for three different Trisonica anemometers and one FT742M (a) standard deviation (b) error (c) sub-optimal sensor placement on-board Aero platform.

from an extended nozzle. We reasoned that if the vapor is unperturbed after exiting the nozzle, then the wind field generated by 4 rotating propellers is practically non-existent. Due to symmetry, the Trisonica was placed at the center of the platform at an arbitrary height of 39cm. A simple air rerouting mechanism was added underneath the exhaust to prevent recirculation by expelling the exhaust laterally downstream with the LCWT airflow. The anemometers were positioned so that the North indicator pointed towards the LCWT. For simplicity, we chose to neglect roll and pitch given that operations are generally done in level attitude with non-aggressive movements. Additionally the Hover1 performs position/altitude hold at $\approx$ 50%-60% of throttle. See Fig. 1 (c) for a view of the experimental setup. Our tests captured data at a sampling rate of 10Hz.

The results from the LCWT shows noisy measurements in both wind speed and direction due to the turbulence from the fans supplying the wind. This can be seen in Fig. 3 where the wind direction in both sensors (including the control) show standard deviations of $\pm\sigma \approx 5^o$. A simple linear regression is used on the median values of the N, E, and D vectors at different throttle positions. From Fig. 4 (a), the average wind speed captured in the N direction is $\sim$3.37$\pm$.407m/s. Though these values fall within the range of the LCWT, the best fit line seems to show a slight increase in measurements for both our control and on-board measurement. Increasing at a rate of 0.23% per unit of throttle input. From Fig. 4 (b), the speed in the E direction is close to zero. This is because it faces perpendicular to the wind and any air circulating from the floor back onto the sensor does not occur. From Fig 4 (c), shows a relatively small slope for the on-board measurement. This would indicate that wind measurements are only slightly perturbed from prop-wash in the up-down direction. Through iterative testing, an optimal location can be chosen which balances the height of the sensor (decreasing the prop wash effect) and maintaining the stability of the aircraft as the configuration is analogous to the inverted pendulum. We reserve this for future work.

The sub-optimal locations for sensor placement on-board the Aero (see Fig. 2 (c)) is constrained by impact areas, other sensor mounting locations, controllability concerns, and obvious prop wash locations. At the center of the fuselage, the prop wash impacts measurements the most causing a 2-3m/s increase in wind speed while at cruising throttle (50%). One location to consider is under the wing in a region close to the fuselage but outside the airflow over the ailerons. In this location it can be also less prone to damage from rough landings.

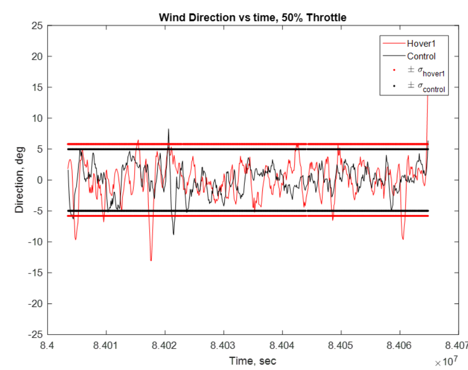

Fig. 3: Trisonica wind direction measurements under operating conditions in LCWT.

V. Estimation Methods

Currently, there has been more work on estimating wind speed and direction on-board fixed-wing aircraft than estimation from the avionics of a VTOL. A recent study by Rhudy et al [8] showed a comparison of estimation techniques using, initially, a GPS and Pitot-static tube and then extend it to include IMU, angle of attack (AOA) and slide-slip angle (SSA) for fixed-wing platforms. Calculating wind speed on VTOL platforms, on the other hand, requires estimation from drag forces [14].

In this work we will look at estimation techniques that require GPS, pitot, and IMU data and exclude methods that use wind vane information for AOA and SSA. Though this can potentially improve the wind estimation [8], the aircrafts used in this study don't have have these built into their designs. Thus, we will investigate methods that use AOA and SSA in future work.

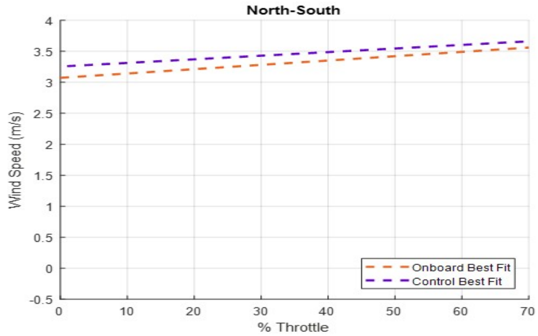

(a)

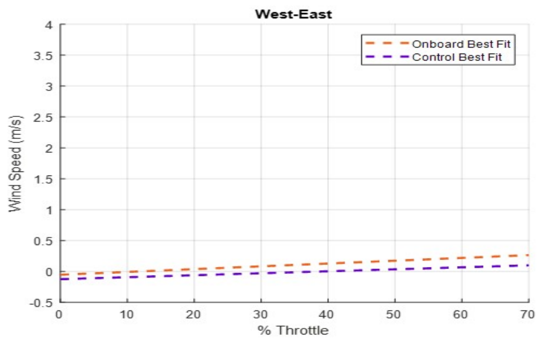

(b)

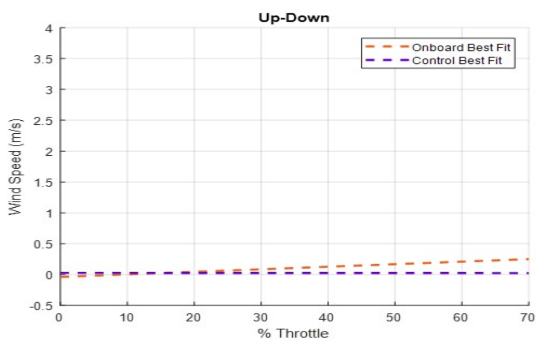

(c)

Fig. 4: Comparison of on-board and control measurements in the (b) N direction (c) E Direction (d) D direction.

These wind estimation techniques require the use of nonlinear state estimation methods such as the Extended Kalman Filter (EKF) or the Sigma-point Kalman Filter (also referred to as the Unscented Kalman Filter (UKF)). Both the EKF and UKF require a nonlinear transformation on the state and observation, $\mathbf{x}_k = f(\mathbf{x}_{k-1}, \mathbf{u}_{k-1}, \mathbf{w}_{k-1})$ and $\mathbf{y}_k = h(\mathbf{x}_k, \mathbf{u}_k, \mathbf{v}_k)$, respectively. Here k refers to the discrete time step, $\mathbf{w}$ is the process noise, and $\mathbf{v}$ is the measurement noise. The EKF is sometimes a more practical choice for state estimation as it is relatively low in computational cost. A disadvantage of the EKF is it requires the calculation of the Jacobian at each time step and a local linear approximation of the nonlinearities. If the Jacobian cannot be calculated sufficiently or the linear approximation is not valid the estimate can become bad and the system will become unstable. The UKF uses a slightly different approach by looking at the mean and covariance of the system and sampling sigma points based on an unscented transformation, which are used to then estimate the state. The unscented transformation calculation at each step can increase the computational cost [15] [3]. The UKF is more desirable for highly nonlinear systems and thus will be used in this work.

A. Method 1

The method described here is based on the work by Cho et al [16] which utilizes the GPS and pitot-static tube measurements along with the flat earth assumption and wind triangle relationship to estimate the wind speed in the north and east directions. The flat earth assumption allows us to consider a Cartesian coordinate system rather than dealing with polar coordinates. The wind triangle relationship can be given as the vector sum of the ground speed and wind to get the airspeed $\mathbf{V}_{air} = \mathbf{V}_{ground} - \mathbf{V}_{wind}$. Let us define the following state variables as, $\mathbf{x} = [\mu_N, \mu_E, \zeta]^T$, $\mathbf{u} = [V_N^{GPS}, V_E^{GPS}]^T$, and $\mathbf{y} = p_d$. Where the state is the wind speed μ and the scale factor ζ and its state dynamics are unknown. Thus, the dynamics are modeled as a random walk, $\mathbf{x}_k = \mathbf{x}_{k-1} + \mathbf{w}_{k-1}$. The process noise is given by $\mathbf{w}$ which has zero mean and covariance matrix $\mathbf{Q}$. By taking the L_2 norm of the wind triangle relationship and defining the scale factor $\zeta = \frac{\rho}{2}\cos^2\alpha \quad \cos^2\beta$. Where ρ is the air density and α and β are the AOA and SSA, respectively. We can write the dynamic pressure, $\mathbf{y} = p_d$, as $\mathbf{y} = \zeta[(V_N^{GPS} - \mu_N)^2 + (V_E^{GPS} - \mu_E)^2] + v_k$.

The measurement input from this method comes from the equation for dynamic pressure $p_d = \frac{\rho}{2}V_{air}^2 + v_{pitot}$ which can be easily calculated from Bernoulli's equation. The measurement noise, $\mathbf{v}$, has zero mean and covariance matrix, $\mathbf{R}$. This measurement along with the state dynamics will be used in the state estimation of the wind.

B. Method 2

An extension to Method 1 by adding down information from the GPS and wind estimation changes the equations as follows, $\mathbf{x} = [\mu_N, \mu_E, \mu_D, \zeta]^T$, $\mathbf{u} = [V_N^{GPS}, V_E^{GPS}, V_D^{GPS}]^T$, and $\mathbf{y} = p_d$. Where p_d for the estimation is given by $\zeta[(V_N^{GPS} - \mu_N)^2 + (V_E^{GPS} - \mu_E)^2 + (V_D^{GPS} - \mu_D)^2] + v_k$ and the measurement p_d is still given by the dynamic pressure from Bernoulli's equation.

C. Method 3

To try and increase the accuracy of the wind estimations, the inertial measurement unit (IMU) input from the accelerometer and gyroscope can be utilized. As Rhudy [8] and Cho [16] mention that including the ground speed information from the GPS into the state can help smooth the GPS signals in the estimation. The state vectors are given as,$\mathbf{x} = [V_N, V_E, V_D, \phi, \theta, \psi, \mu_N, \mu_E, \mu_D, \zeta]^T$, $\mathbf{u} = [a_x, a_y, a_z, p, q, r]^T$, and $\mathbf{y} = [V_N, V_E, V_D, p_d]^T$. The attitude roll, pitch, and yaw are denoted as ϕ, θ, and ψ. The accelerometer data in the x, y, and z directions are given by the a. The roll, pitch, and yaw rates are given by p, q, and r.

In order to use this new formulation for the state equations we need to rotate the data into the global frame for the velocities, $\dot{V}_i$ and the attitude rates $\dot{\phi}$, $\dot{\theta}$, and $\dot{\psi}$.

$$\begin{bmatrix}\dot{V}_N\\ \dot{V}_E\\ \dot{V}_D\end{bmatrix} = DCM(\phi,\theta,\psi)\Big(\begin{bmatrix}a_x\\ a_y\\ a_z\end{bmatrix} + \mathbf{w}_a\Big) - \begin{bmatrix}0\\ 0\\ g\end{bmatrix} \quad (1)$$

$$\begin{bmatrix}\dot{\phi}\\ \dot{\theta}\\ \dot{\psi}\end{bmatrix} = \begin{bmatrix}1 & \sin\phi\tan\theta & \cos\phi\tan\theta\\ 0 & \cos\phi & -\sin\phi\\ 0 & \sin\phi\sec\theta & \cos\phi\sec\theta\end{bmatrix}\Big(\begin{bmatrix}p\\ q\\ r\end{bmatrix} + \mathbf{w}_\omega\Big) \quad (2)$$

The direct cosine matrix $DCM(\phi, \theta, \psi)$ translates from body fixed from to the inertial frame. All the process noise $\mathbf{w} = [\mathbf{w}_a \;\; \mathbf{w}_\omega \;\; \mathbf{w}_\mu]^T$ and measurement noise $\mathbf{v} = [\mathbf{v}_{GPS} \; v_{pitot}]^T$ are specific to the equipment you are using. If the noise is not accounted for properly the estimation algorithm does not work very well.

D. Method 4

The last method we will explore is based on drag force for VTOL platforms. The avionics and its response to the tilt from drag force is utilized to estimate wind. Xiang et al[14] explore a few different approaches, namely: a Kalman filter, Simple method and Linear method. Since their Simple method deviated from the results obtained in the Kalman filter and Linear method approach we are going to explore the Linear model here. It is formulated as follows,

$$\begin{aligned} D_x &= (\cos\psi\sin\theta\cos\phi)T - \ddot{x}m \\ D_y &= (\sin\psi\sin\theta\cos\phi)T - \ddot{y}m \\ D_z &= (\cos\theta\cos\phi)T - \ddot{x}m - gm \end{aligned} \quad (3)$$

Where D is the drag force ($D = \sqrt{D_x^2 + D_y^2}$) and the equations in (3) are expanded from the product of the DCM and the thrust vector $T = [0, 0, T]^T$. This implies there is no pitch or roll inputs on the aircraft. If the vertical movement is small the drag on the z-component can be assumed zero. Then the thrust can be solved for, $T = \frac{(\ddot{z}+g)m}{\cos\theta\cos\phi}$. Once the drag is calculated the tilt angle γ can be related to the pitch and roll angles by the following,

$$|\mu| = \sqrt{\frac{2D}{\rho A(\gamma)C_D(\gamma)}}, \quad \gamma = \cos^{-1}\frac{\vec{u}_{xy}\cdot(\vec{e}_\phi \times \vec{e}_\theta)}{|\vec{u}_{xy}|\cdot|(\vec{e}_\phi \times \vec{e}_\theta)|} \quad (4)$$

$$\vec{e}_\phi = \begin{bmatrix}0\\ \cos\phi\\ \sin\phi\end{bmatrix} \quad , \quad \vec{e}_\theta = \begin{bmatrix}\cos\theta\\ 0\\ -\sin\theta\end{bmatrix} \quad (5)$$

where $\vec{u}_{xy}$ is the unit vector normal to the xy plane, e_θ and e_ϕ are unit vectors pointing in the pitch and roll directions, and $|\mu|$ is the drag based velocity. The velocity can be then equated as a function of γ. Note, the cross-sectional area $A(\gamma)$ and drag coefficient $C_d(\gamma)$ are platform specific functions of γ that need to be determined. The direction of the wind can be calculated from angle λ and the sign of $\vec{u}_{xz}\cdot(\vec{e}_\phi \times \vec{e}_\theta)_{xy}$.

$$\lambda = \psi - tan^{-1}\frac{(\vec{e}_\phi \times \vec{e}_\theta)_y}{(\vec{e}_\phi \times \vec{e}_\theta)_x} \quad (6)$$

$$D_\mu = \begin{cases} 360\deg - \lambda + \phi, & \vec{u}_{xz}\cdot(\vec{e}_\phi \times \vec{e}_\theta)_{xy} > 0 \\ \lambda + \phi, & \vec{u}_{xz} > 0 \end{cases}$$

TABLE II: Measurement noise and state estimation uncertainties used in wind estimation methods.

parameter	source	variable	σ noise
attitude	EKF in autopilot	ϕ, θ, ψ	0.067
airspeed	pitot (DPS)	V_{air}	0.718
ground speed	GPS unit	V_N^{GPS},V_E^{GPS},V_D^{GPS}	0.315
acceleration	IMU unit	a_x,a_y,a_z	0.067
angular rate	IMU unit	p, q, r	0.067
wind	state variable	μ_N, μ_E, μ_D	0.22

VI. Experiment

To compare the measurements on-board the fixed-wing and VTOL platforms with the estimation techniques (Section V) we conducted flights from both sUAS simultaneously. Two Trisonica-Mini's were attached to sUAS (as per Section IV) and the FT742SM due to its weight was not considered for placement on either platform.

Trisonica (T1) is attached to the Hover1 at 39cm and will be referred to as "Hover". The second Trisonica (T3) is placed underneath the portside wing of the Aero with an equally weighted counterbalance placed opposite on the starboard side, referred to as "Aero". The experiment consists of 3 flights with 3 different flight patterns for the Aero at an altitude of 30m AGL. The Hover1 will be maintained in a position hold mode (to satisfy assumptions in method 4) at an equal altitude as the Aero during all three flights. The weather station (KMCE) data is shown in Fig. 8 for the day. The flights took place between 7-8:00pm at UC Merced's Vernal Pools & Grassland Reserve in the evening with fairly stable wind speeds. The two first flights for the Aero consisted of a lawn mower pattern with long legs running perpendicular and parallel to the wind. The last flight of the Aero consists of a circular flight pattern at a 60m radius. These flight patterns are chosen to examine the effects of flight path on estimation algorithms but more importantly to examine the effects of measurements on-board the Aero. The actual flight paths and experiment location can be seen in Fig. 8.

VII. Results

In section IV we explored the effects of prop wash on sensor readings of the VTOL. We can calculate the difference in these measurement readings by taking into consideration the changes in the NED direction velocities as a function of throttle position, $\mathbf{V}_{wind}^{corrected} = \mathbf{V}_{wind} - \Delta\mathbf{V}_{wind}$.

$$\Delta\mathbf{V}_{wind} = \Delta V_N\hat{N} + \Delta V_E\hat{E} + \Delta V_D\hat{D}$$

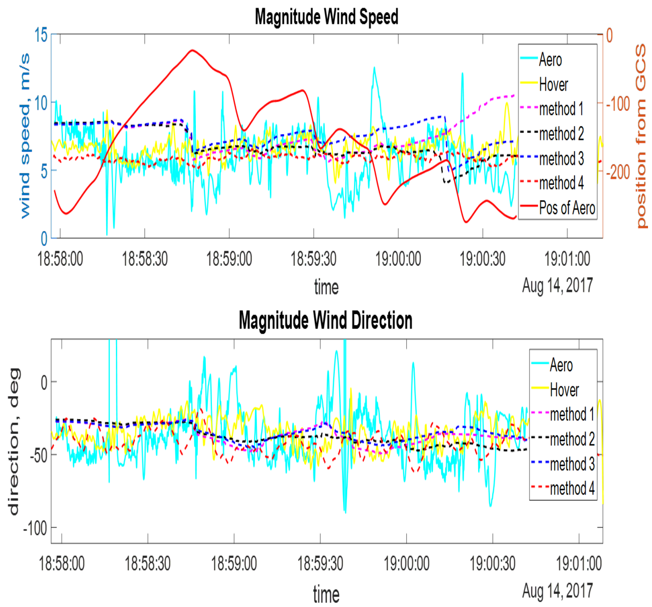

Fig. 5: Wind measurement and estimation for perpendicular lawn-mower flight path.

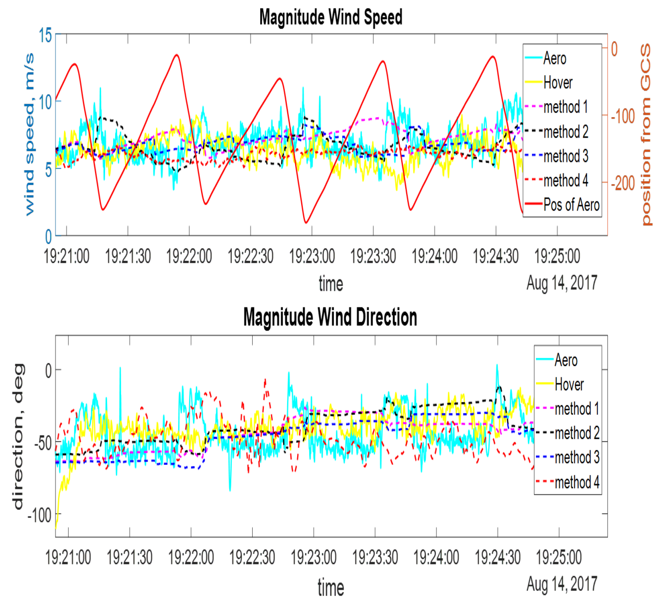

Fig. 6: Wind measurement and estimation for parallel lawn-mower flight path.

In our case the changes in velocity where small ($\approx$ 0.2m/s, see Fig. 4). The control and on-board measurements for the North and East directions are approximately parallel and positive in their slope. This may suggest that propellers are influencing the airflow of the room changing the inlet conditions of the LCWT and the airspeed to the control. However, the Down direction has a different trend. The control curve is relatively flat with a positive slope for the on-board measurement. Even though this difference exists, it is quite small (within standard deviation of the sensors capabilities). Thus there is no distinguishable or clear prop wash effect on the measurements taken at 39cm. With limitations on our LCWT speeds, we are restricted to only being able to comment on airspeeds of $\approx$ 3.4m/s. Moreover, we also suspect that vibration induced noise may influence measurements as well. The amount of vibration will depend of course on different material stiffness of the pole used and how the aircraft is being flown.

The results from the 3 flight experiments for the Aero and Hover can be seen in Fig. 8. Each set of measured and estimated wind flight data can be seen in Fig. 5-7 where the measured quantities are shown in cyan and yellow for the Aero and Hover, respectively. The estimation techniques for the Aero are given by methods 1-3 shown in magenta, black and blue (dotted lines). The estimation technique for the Hover is given by method 4 in red (dotted line). The position of the Aero from the ground control station (GCS) facing the wind is shown in red (solid). The wind conditions where relatively stable with little variance and decreased in speed from $\approx$ 10 m/s when we first arrived on site to $\approx$ 5-7 m/s during the experiment (see Fig 9).

The Hover was compared with only one estimation technique in this work under the assumption that the pitch and roll components are relatively small. This was the approximation made in determining the wind speed and direction in Section V. The wind speed estimated and the wind speed measured during these three flights were consistent between the two. The velocity and direction components aligned rather well with only subtle discrepancies. The differences could be attributed do to vibration and alignment mismatch between the sensor and the aircraft. Also, the Trisonica seems to be much more sensitive to subtle changes and noise whereas the estimation is not. This can possibly be explained by how the IMU is filtering the data before it is used in estimation as well as how sensitive the IMU is.

The Aero was compared to three estimation techniques over three different flight paths (perpendicular, parallel, and circular). Like the Hover results, the Trisonica shows noise in its measurements. The first flight path (Fig. 5) shows the most noise when the aircraft turns left into the wind. Since the sensor is placed on the left (port-side) of the aircraft it suggests that the placement is interfering with the measurements. This is best seen on flight 3 (Fig 7) where the circular path is executed in a anti-clockwise manor. Fig 6 also shows distinct shifts in direction during the right hand turns going downwind. This opens up the left side of the aircraft to the wind. It should also be noted that during these maneuvers, especially the perpendicular flight, that the aggressiveness can affect the estimation. We see that towards the end of flight 1 (perpendicular) that the wind direction estimation becomes particularly bad compared to the other flights. The erratic nature of the aircraft turning on a crosswind leg may cause the noise parameters to increase. Thus, depending on the flight plan/conditions and the initial noise parameters chosen (for your specific aircraft used), the UKF formulation needs to be evaluated prior to provide the best results.

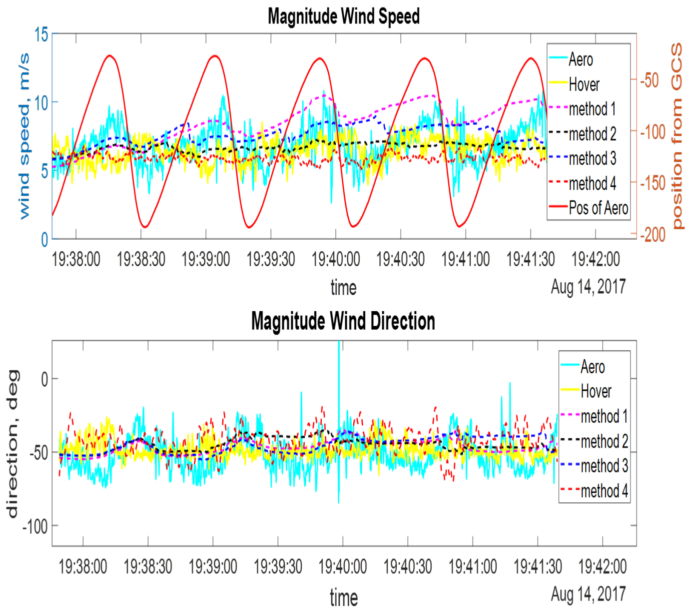

Fig. 7: Wind measurement and estimation for circular flight path radius 60m.

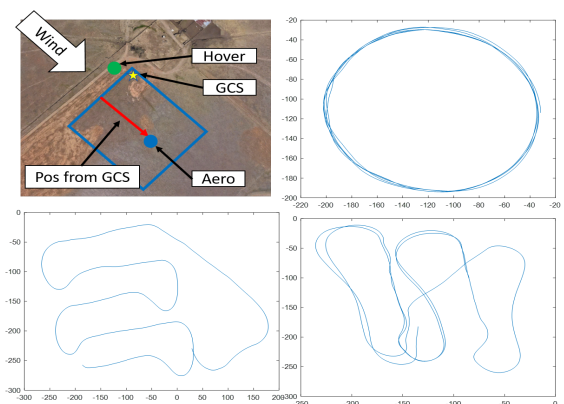

Fig. 8: Experiment flight paths and relative wind direction at test site.

Method 3 was shown by [8] to agree the most with the weather station data on their experiment. This method (black dotted line) shows good agreement with the Hover measurements (yellow) and estimations (red dotted). This suggests that the use of measurements on-board the Hover a reasonably sufficient. This also provides a sort of confirmation that the estimation on the Hover is reliable as well. While, the differences they share could be attributed to experiencing different local turbulences as they are not in the same location. The spatial and temporal characteristics of the wind seen at these different locations prevent us from achieving good ground truths. This can even be the case with corrected power law measurements from local weather station data.

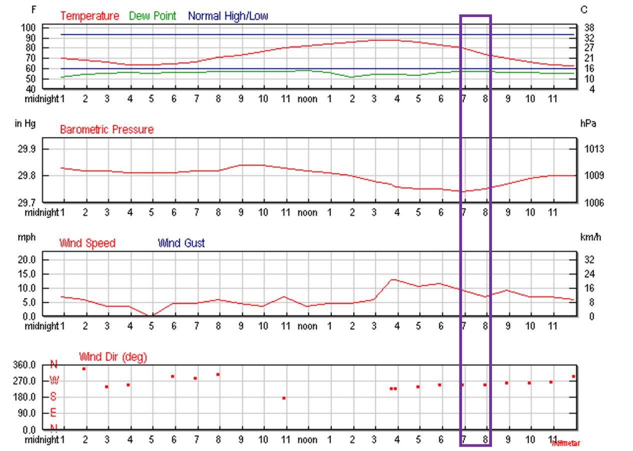

Fig. 9: Experiment weather data from KMCE weather station located 8 miles from testing site at UC Merced Vernal Pool Reserve.

VIII. Conclusion & Future Work

In this paper we have compared the FT742-SM and Trisonica Mini anemometers in a Aerolab EWT for accuracy, we have shown that prop wash effect can be negligible for measurements on-board VTOL platforms (39cm for our case) at airspeeds of 3.4 m/s in our LCWT, and we have tested the Trisonica Mini anemometers on-board the two UAS's (VTOL and fixed-wing) against their respective estimation techniques. We conclude that it is possible to measure and estimated on-board the VTOL when pitch and roll angles are small. Future work will attempt to incorporate different height placements as well as consider roll/pitch on-board the Hover for optimal placement. We observed the Aero has noisy measurements depending on crosswind aerodynamics. We believe this to be caused by the sensor location. Future work will look to change the sensor placement on the Aero in order to reduce the aerodynamic effects of crosswind airflow around the body to improve measurements.

Acknowledgment

We would like to thank Gordon Bease from FT Technologies for the equipment and interest in our problem and our undergraduates for their help with running experiments: Alexis Bonnin, Asia Chi, Tomny Hang, and Joshua Ahmed. We also thank the reviewers for helpful comments in improving the quality and presentation of the paper.

References

[1] B. Smith, G. John, B. Stark, L. E. Christensen, and Y. Chen, "Applicability of unmanned aerial systems for leak detection," *International Conference on Unmanned Aircraft Systems*, 2016.

[2] P. Bruschi, M. Piotto, F. Dell'Agnello, J. Ware, and N. Roy, "Wind speed and direction detection by means of solid-state anemometers embedded on small quadcopters.," *Procedia Engineering Eurosensors Conference*, vol. 168, pp. 802–805, 2016.

[3] R. Beard and T. McLain, *Small Unmanned Aircraft: Theory and Practice*. Princeton, New Jersey: Princeton University Press, 2012.

[4] J. Langelaan, "Wind field estimation for small unmanned aerial vehicles," *AIAA Guidance, Navigation and Control Conference*.

[5] K. T. Borup, T. I. Fossen, and T. A. Johansen, "A nonlinear model-based wind velocity observer for unmanned aerial vehicles," *International Federation of Automatic Control*, 2016.
[6] T. A. Johansen, A. Cristofaro, K. Sorensen, J. M. Hansen, and T. I. Fossen, "On estimation of wind velocity, angle-of-attack and sideslip angle of small UAVs using standard sensors," *International Conference on Unmanned Aircraft Systems*, 2015.
[7] M. B. Rhudy, M. L. Fravolini, Y. Gu, M. R. Napolitano, S. Gururajan, and H. Chao, "Aircraft model-independent airspeed estimation without pitot tube measurements," *IEEE Transactions on Aerospace and Electronic Systems*, vol. 51, no. 3, pp. 1980–1995, 2015.
[8] M. Rhudy, Y. GU, J. Gross, and H. Chao, "Onboard wind velocity estimation comparison for unmanned aircraft systems," *IEEE TRANSACTIONS ON AEROSPACE AND ELECTRONIC SYSTEMS*, vol. 53, no. 1, pp. 55–66, 2017.
[9] A. Wenz and T. A. Johansen, "Estimation of wind velocities and aerodynamic coefficients for uavs using standard autopilot sensors and a moving horizon estimator," *International Conference on Unmanned Aircraft Systems*, 2017.
[10] J. Newman and P. M. Klein, "The impacts of atmospheric stability on the accuracy of wind speed extrapolations," *Resources*, vol. 3, pp. 81–105, 2014.
[11] J. Peichl, A. Karion, C. Sweeney, E. A. Kort, M. L. Smith, A. R. Brandtl, T. Yekoo, K. C. Aikin, S. A. Conley, A. Gvakharia, M. Trainer, S. Wolter, and T. B. Ryerson, "Quantifying atmospheric methane emissions from oil and natural gas production in the bakkan shale region of north dakota," *Journal of Geophysical Research: Atmospheres*, vol. 121, pp. 6101–6111, 2015.
[12] Anemoment, "Trisonica mini comparison," *http://www.anemoment.com*, 2018.
[13] F. Technologies, "Ft742," *http://www.fttechnologies.com*, 2018.
[14] X. Xiang, Z. Wang, Z. Mo, G. Chen, E. Blasch, and K. Pham, "Wind field estimation through autonomous quadcopter avionics," *IEEE*, 2016.
[15] M. Rhudy and Y. Gu, "Understanding nonlinear kalman filters, part ii: an implementation guide," *Interactive Robotics Letters, West Virginia University*.
[16] A. Cho, J. Kim, S. Lee, and C. Kee, "Wind estimation and airspeed calibration using a uav with a single antenna gps receiver and pitot tube," *IEEE Transactions on Aerospace and Electronic Systems*, vol. 47, no. 1, pp. 109–117, 2011.